

## Design, Synthesis, and Biological Evaluation of a Novel Class of $\gamma$ -Secretase Modulators with PPAR $\gamma$ Activity

Martina Hieke,<sup>†</sup> Julia Ness,<sup>‡</sup> Ramona Steri,<sup>†</sup> Michaela Dittrich,<sup>†</sup> Christine Greiner,<sup>§</sup> Oliver Werz,<sup>§</sup> Karlheinz Baumann,<sup>||</sup> Manfred Schubert-Zsilavecz,<sup>†</sup> Sascha Weggen,<sup>\*,‡</sup> and Heiko Zettl<sup>\*,†,⊥</sup>

<sup>†</sup>Institute of Pharmaceutical Chemistry, ZAFES/LiFF/Goethe University Frankfurt, Max-von-Laue-Strasse 9, D-60438 Frankfurt am Main, Germany, <sup>‡</sup>Molecular Neuropathology Group, Department of Neuropathology, Heinrich-Heine University Duesseldorf, Moorenstrasse 5, D-40225 Duesseldorf, Germany, <sup>§</sup>Department of Pharmaceutical Analytics, Eberhard-Karls University Tuebingen, Auf der Morgenstelle 8, D-72076 Tuebingen, Germany, and <sup>||</sup>Pharmaceuticals Division, Preclinical Research CNS, F. Hoffmann-La Roche Ltd., CH-4070 Basel, Switzerland. <sup>⊥</sup>Present address: ETH Zurich, Institute of Pharmaceutical Sciences, Wolfgang-Pauli-Strasse 10, CH-8093 Zurich, Switzerland.

Received March 8, 2010

We present a novel class of dual modulators of  $\gamma$ -secretase and peroxisome proliferator-activated receptor  $\gamma$  (PPAR $\gamma$ ) based on the structure of 2-(bis(phenethoxy)pyrimidine-2-ylthio)hexanoic acid **8** (IC<sub>50</sub>(A $\beta$ 42) = 22.8  $\mu$ M, EC<sub>50</sub>(PPAR $\gamma$ ) = 8.3  $\mu$ M). The modulation of both targets with approved drugs (i.e., amyloid- $\beta$  42 (A $\beta$ 42)-lowering NSAIDs for  $\gamma$ -secretase and glitazones for PPAR $\gamma$ ) has demonstrated beneficial effects in in vitro and in vivo models of Alzheimer's disease (AD). However, although NSAIDs and PPAR $\gamma$  agonists share similar structural features, no druglike compounds with dual activities as  $\gamma$ -secretase modulators (GSMs) and PPAR $\gamma$  agonists have been designed so far. On the basis of our initial lead structure **8**, we present the structure–activity relationships (SARs) of broad structural variations. A significant improvement was reached by the introduction of *p*-trifluoromethyl substituents at the phenyl residues yielding compound **16** (IC<sub>50</sub>(A $\beta$ 42) = 6.0  $\mu$ M, EC<sub>50</sub>(PPAR $\gamma$ ) = 11.0  $\mu$ M) and the replacement of the two phenyl residues of **8** by cyclohexyl yielding compound **22** (IC<sub>50</sub>(A $\beta$ 42) = 5.1  $\mu$ M, EC<sub>50</sub>(PPAR $\gamma$ ) = 6.6  $\mu$ M).

### Introduction

Alzheimer's disease (AD<sup>a</sup>) is the most common age-related cause of dementia with 26.6 million patients worldwide in 2006 and over a 100 million predicted cases by 2050.<sup>1</sup> The cardinal symptom of the disease is progressive memory loss due to the degeneration of neurons and synapses in the cerebral cortex and subcortical regions of the brain. The neuropathology of AD is characterized by the extracellular deposition of amyloid- $\beta$  (A $\beta$ ) plaques, the formation of intracellular neurofibrillary tangles, chronic brain inflammation, and oxidative damage.<sup>2</sup> According to the modified amyloid hypothesis, small soluble oligomers of A $\beta$  peptides, particularly those formed by the highly hydrophobic A $\beta$ 42 species, are the disease-initiating agents in AD.<sup>3</sup> A $\beta$ 42 is a proteolytic fragment resulting from sequential cleavage of the amyloid precursor protein (APP) by two aspartyl proteases, i.e.,  $\beta$ -secretase and  $\gamma$ -secretase. Currently, a variety of potentially disease-modifying therapeutic approaches are under development that target the production, aggregation, or clearance of A $\beta$  peptides in brain (Scheme 1).<sup>4,5</sup> Substantial advances have been made with respect to inhibitors of the

$\gamma$ -secretase enzyme, a multiprotein complex that catalyzes the final step in the cellular generation of A $\beta$  peptides. However, because of its essential role in the NOTCH signaling pathway, mechanism-based toxicity with severe phenotypes in the gastrointestinal and hematopoietic systems has been observed in preclinical studies of  $\gamma$ -secretase inhibitors<sup>6–8</sup> and might be a limiting factor in clinical efficacy. Intriguingly, a subset of nonsteroidal anti-inflammatory drugs (NSAIDs) such as ibuprofen and indomethacin were found to modulate the  $\gamma$ -secretase activity in a way that allowed selective inhibition of A $\beta$ 42 production (Figure 1).<sup>9</sup> These compounds, termed  $\gamma$ -secretase-modulators (GSMs), shifted the proteolytic processing of APP toward higher production of shorter A $\beta$  species such as A $\beta$ 38 at the expense of the highly toxic A $\beta$ 42. Importantly, impairment of NOTCH processing and signaling was not observed.<sup>9,10</sup> Unfortunately, these NSAID-type GSMs suffer from low potency against  $\gamma$ -secretase (Figure 1), poor brain permeability, and side effects related to inhibition of cyclooxygenases (COX) such as gastrointestinal toxicity and increased cardiovascular mortality.<sup>11</sup> Consequently, NSAID-type GSMs and derived analogues, whose consumption appeared to confer a reduced risk for AD in epidemiological studies, have produced negative or inconclusive clinical results in patients suffering from established AD<sup>11–14</sup> or showed unacceptable side effects for long-term treatment. Recently, potent GSMs with favorable pharmacological properties have emerged.<sup>15,16</sup>

In addition, some NSAIDs including the GSMs indomethacin and ibuprofen function as agonists of the peroxisome

\*To whom correspondence should be addressed. For S.W.: phone, +49 (211) 8104506; fax, +49 (211) 8104577; e-mail, sweggen@uni-duesseldorf.de. For H.Z.: phone, +41 (44) 6339113; fax, +41 (44) 6331379; e-mail, heiko.zettl@pharma.ethz.ch.

<sup>a</sup> Abbreviations: A $\beta$ , amyloid  $\beta$  peptide; AD, Alzheimer's disease; APP, amyloid precursor protein; COX, cyclooxygenase; GSM,  $\gamma$ -secretase modulator; NSAIDs, nonsteroidal anti-inflammatory drugs; PPAR, peroxisome proliferator-activated receptor; SAR structure–activity relationship.

Scheme 1. Amyloid Cascade

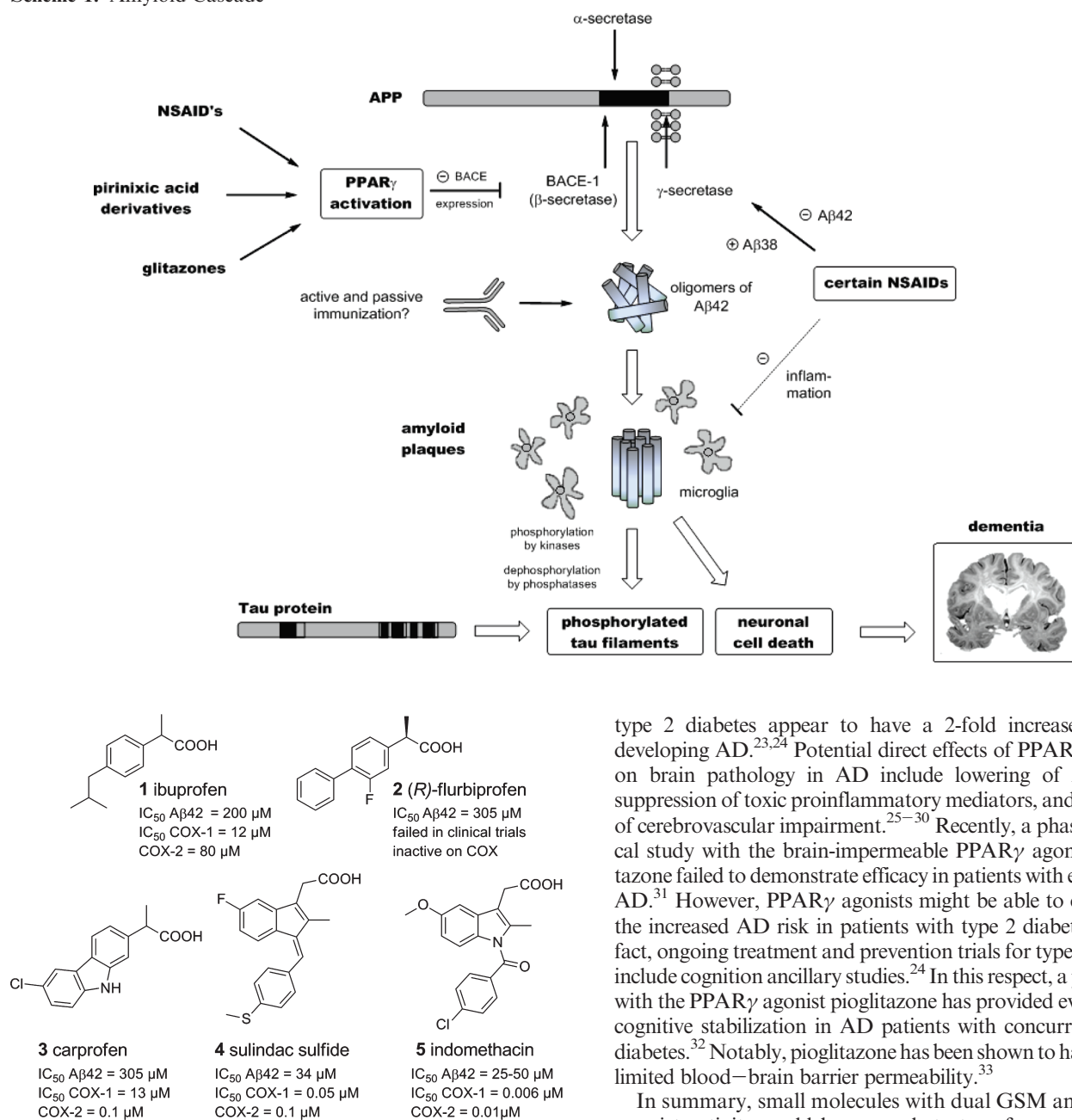


**Figure 1.** In vitro pharmacology of  $\gamma$ -secretase-modulating NSAIDs.<sup>15,47–49</sup>

proliferator-activated receptor  $\gamma$  (PPAR $\gamma$ ).<sup>17,18</sup> PPAR $\gamma$  belongs to a family of ligand-activated nuclear receptors that act as lipid sensors, and synthetic ligands for PPAR $\gamma$  include the widely prescribed antidiabetic drugs rosiglitazone and pioglitazone.<sup>19</sup> Evidence indicates that PPAR $\gamma$  agonists might have multiple beneficial effects in AD both on core pathological processes in brain and on peripheral factors such as serum glucose levels and insulin sensitivity that constitute potential risk factors for AD.<sup>20</sup> Several studies have demonstrated that AD is associated with perturbations in insulin metabolism, and diet-induced insulin resistance caused increased brain  $A\beta$  levels and plaque formation in a mouse model of AD.<sup>21</sup> In addition, a recent cross of an AD mouse model to leptin-deficient diabetic mice revealed accelerated learning deficits and severe cerebrovascular amyloid deposition.<sup>22</sup> Importantly, individuals with

type 2 diabetes appear to have a 2-fold increased risk of developing AD.<sup>23,24</sup> Potential direct effects of PPAR $\gamma$  agonists on brain pathology in AD include lowering of  $A\beta$  levels, suppression of toxic proinflammatory mediators, and reduction of cerebrovascular impairment.<sup>25–30</sup> Recently, a phase III clinical study with the brain-impermeable PPAR $\gamma$  agonist rosiglitazone failed to demonstrate efficacy in patients with established AD.<sup>31</sup> However, PPAR $\gamma$  agonists might be able to counteract the increased AD risk in patients with type 2 diabetes, and in fact, ongoing treatment and prevention trials for type 2 diabetes include cognition ancillary studies.<sup>24</sup> In this respect, a pilot study with the PPAR $\gamma$  agonist pioglitazone has provided evidence for cognitive stabilization in AD patients with concurrent type 2 diabetes.<sup>32</sup> Notably, pioglitazone has been shown to have at least limited blood–brain barrier permeability.<sup>33</sup>

In summary, small molecules with dual GSM and PPAR $\gamma$  agonist activity could be a novel strategy for prevention of AD, particularly in patients with type 2 diabetes. In an initial screening of our in-house compound library, we have identified compound **8** (2-(bis(phenethoxy)pyrimidine-2-ylthio)hexanoic acid) that displayed a typical GSM profile and concentration-dependently and selectively decreased  $A\beta_{42}$  levels with a concomitant increase in  $A\beta_{38}$  production ( $IC_{50}$ -( $A\beta_{42}$ ) = 22.8  $\mu$ M,  $EC_{50}$ ( $A\beta_{38}$ ) = 11.3  $\mu$ M, Figure 2). Additionally, compound **8** is a subtype-selective PPAR $\gamma$  modulator ( $EC_{50}$  = 8.3  $\mu$ M, 60% max activation). Here, we describe the structure–activity relationships (SARs) of a novel class of dual  $\gamma$ -secretase/PPAR $\gamma$  modulators based on the scaffold of compound **8**. Our strategy aimed at improving the GSM activity while maintaining PPAR $\gamma$  agonism. Characteristic structural features of compound **8** are a carboxylic acid headgroup and two phenethyl residues forming a lipophilic backbone. As conventional NSAIDs have similar structural features, we further determined the inhibitory activity of all compounds for COX-1 and COX-2.

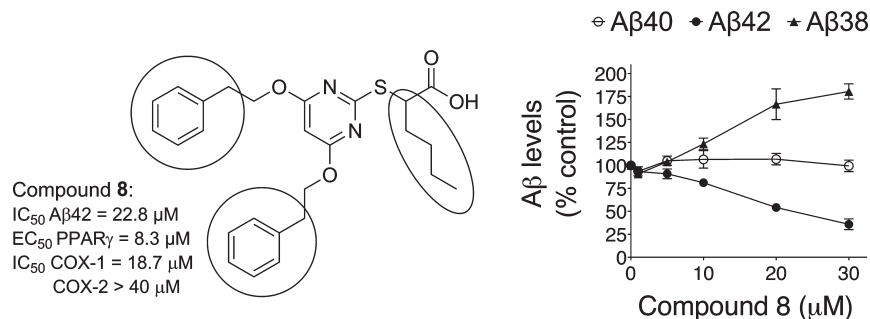
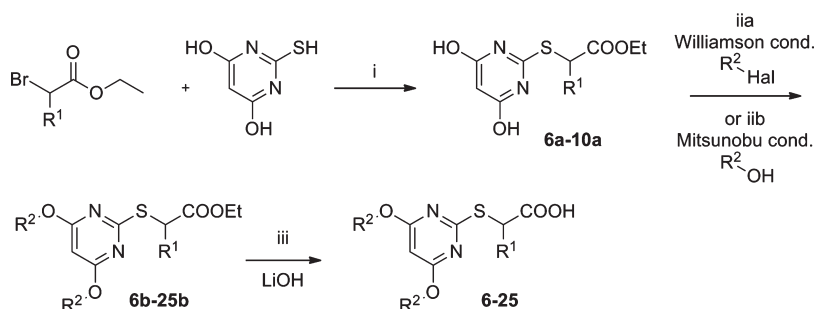


**Figure 2.** Lead compound **8** and its impact on A $\beta$ 38, A $\beta$ 40, and A $\beta$ 42 formation. SARs based on **8** were obtained by structural modifications of the encircled residues.

### Scheme 2. Synthetic Route of Compounds 6–25<sup>a</sup>



<sup>a</sup> Reagents and conditions: (i) 2-bromo-( $R^1$ )-ethyl acetate (1.5 equiv), thiobarbituric acid (1 equiv), TEA (1.5 equiv), DMF, 80 °C, 4 h; (ii) **6a–10a** (1 equiv),  $R^2$ -Hal (2.1 equiv),  $K_2CO_3$  (2.3 equiv), DMF, 80 °C, 3–28 h or (iib) **6a–10a** (1 equiv),  $R^2$ -OH (2 equiv), DEAD (2.5 equiv), TPP (2.5 equiv), THF, room temp, 1–3 h; (iii) LiOH (5 equiv), THF/MeOH,  $H_2O$ , 25–50 °C, 2–24 h.

### Chemistry

The general synthetic procedure of the compounds is illustrated in Scheme 2. Presented compounds were prepared in a three-step reaction, which has been described previously by Koeberle et al.<sup>34</sup> First, a nucleophilic substitution between thiobarbituric acid and the respective  $\alpha$ -bromoethyl ester using dimethylformamide (DMF) as solvent and triethylamine (TEA) as corresponding base was carried out. This step was followed by the etherification of the two hydroxyl groups, either by a Mitsunobu reaction or by a Williamson ether synthesis. In the case of the Mitsunobu reaction, we used the precursor, the respective alcohol, triphenylphosphine (TPP), and diethylazodicarboxylate (DEAD) and stirred the solution at room temperature under argon atmosphere.<sup>35</sup> The Williamson ether synthesis was carried out with the respective alkyl halogenide,  $K_2CO_3$ , and DMF at 80 °C. Finally, the ester group was hydrolyzed with LiOH in tetrahydrofuran (THF) and  $H_2O$  to yield final compounds **6–25**.

### Biological Assays

PPAR activity of the final compounds was tested in a cellular luciferase-based PPAR transactivation assay, which has been described previously.<sup>36</sup> Final compounds **6–25** were fully characterized on all PPAR subtypes ( $\alpha$ ,  $\gamma$ , and  $\delta$ ). Since every derivative described in this paper was inactive on PPAR $\alpha$  and PPAR $\delta$  (tested concentration of 10  $\mu M$ ), the following discussion is only focused on PPAR $\gamma$  activity. For biological characterization of GSM activity, we measured the levels of A $\beta$ 38, A $\beta$ 40, and A $\beta$ 42 peptides in cell supernatants with an ELISA assay as described with some modifications.<sup>37</sup> Inhibition of COX was tested in a cell-free assay using isolated ovine COX-1 and human recombinant COX-2 enzymes.<sup>34</sup>

Potential effects on proteolytic processing of NOTCH were investigated for the two compounds with the highest GSM activity using a previously described reporter assay.<sup>38</sup> Cytotoxicity of all compounds was determined using alamar blue reagent.

### Results

In an initial screening of our in-house-library we have identified 2-(bis(phenethoxy)pyrimidine-2-ylthio)hexanoic acid **8**, a selective PPAR $\gamma$  modulator that displayed the characteristic GSM activity with  $IC_{50}(A\beta_{42}) = 22.8 \mu M$  (Figure 2). As the first hit, compound **8** served as the structural template for all presented derivatives. Important structural features of **8** are two 2-phenethyl residues forming a lipophilic backbone and a carboxylic acid function as headgroup. This acidic headgroup is an essential structural element required for PPAR $\gamma$  activation<sup>39</sup> and of NSAID-type GSMs.<sup>15,40</sup> Therefore, we have not modified the carboxylic acid group and focused our efforts on the remaining parts of lead structure **8**.

In previous studies, we have observed that the length of the alkyl chain of  $\alpha$ -substituted pirinixic acid derivatives has a high impact on PPAR activity.<sup>41,42</sup> Hence, we systematically varied this position by elongation and shortening of the  $\alpha$ -*n*-butyl residue as well as by introduction of a  $\alpha$ -phenyl residue (compounds **6–10**; see Table 1). The inhibitory activity on A $\beta$ 42 production showed clear SAR depending on the length of the  $\alpha$ -alkyl chain. Removal of the  $\alpha$ -chain (compound **6**,  $R^1 = H$ ) caused a complete loss of GSM activity. In line with this observation, compound **7** with the shorter ethyl residue showed only weak GSM activity ( $IC_{50}(A\beta_{42}) = 41.6 \mu M$ ). A slight decrease of GSM activity was also observed after elongation to *n*-hexyl (compound **9**). In regard to PPAR $\gamma$

**Table 1.** PPAR $\gamma$  Activation and  $\gamma$ -Secretase Modulation (Determined by A $\beta$ 42 Inhibition and A $\beta$ 38 Activation) of Compounds 6–25<sup>a</sup>

Compound			PPAR $\gamma$ activation		$\gamma$ -secretase modulation	
	R <sub>1</sub>	R <sub>2</sub>	EC <sub>50</sub> in $\mu$ M $\pm$ SD	Maximal activation in [%] $\pm$ SD	Inhibition of A $\beta$ 42 (IC <sub>50</sub> in $\mu$ M)	Activation of A $\beta$ 38 (EC <sub>50</sub> in $\mu$ M)
<b>Variation of <math>\alpha</math>-substitution</b>						
<b>6</b>	-H		3.7 $\pm$ 1.0	111 $\pm$ 22	> 40	> 40
<b>7</b>			6.1 $\pm$ 0.2	57 $\pm$ 2	41.6	31.1
<b>8</b>			8.3 $\pm$ 0.1	61 $\pm$ 1	22.8	11.3
<b>8c</b>			22% @10 $\mu$ M		21.5	8.4
<b>8d</b>			10.4 $\pm$ 0.4	62 $\pm$ 3	32.6	13.5
<b>9</b>			8.8 $\pm$ 0.4	59 $\pm$ 5	30.4	24.2
<b>10</b>			Inactive		29.3	12.8
<b>Variation of alkyl spacer</b>						
<b>11</b>			31% @ 20 $\mu$ M		25.2	24.2
<b>12</b>			8.9 $\pm$ 2.1	71 $\pm$ 14	30.9	16.4
<b>13</b>			10.0 $\pm$ 1.2	55 $\pm$ 7	22.9	16.4
<b>Introduction of para-substituents</b>						
<b>14</b>			7.5 $\pm$ 1.4	63 $\pm$ 17	13.0	6.4
<b>15</b>			23% @10 $\mu$ M		19.3	6.2
<b>16</b>			11.0 $\pm$ 0.3	112 $\pm$ 2	6.0	1.8
<b>17</b>			10.3 $\pm$ 1.6	115 $\pm$ 21	8.6	5.5
<b>18</b>			33% @ 6 $\mu$ M		31.2	Not determined
<b>19</b>			7.0 $\pm$ 0.9	65 $\pm$ 7	> 40	Not determined
<b>20</b>			32% @10 $\mu$ M		37.7	17.5
<b>Introduction of aliphatic residues</b>						
<b>21</b>			Inactive		11.3	1.9
<b>22</b>			6.6 $\pm$ 0.4	71 $\pm$ 5	5.1	4.6
<b>23</b>			12.1 $\pm$ 0.2	127 $\pm$ 2	17.2	9.0
<b>24</b>			4.3 $\pm$ 0.9	79 $\pm$ 8	> 40	24.0
<b>25</b>			11.0 $\pm$ 0.1	69 $\pm$ 1	28.2	10.9

<sup>a</sup> Inactive: tested concentration of 10  $\mu$ M.

activation, the length of the  $\alpha$ -alkyl chain did not considerably influence the activity (EC<sub>50</sub> values of 6–9 between 3 and 9  $\mu$ M,

with a tendency for decreased activity with longer chains). Phenyl-substituted **10** showed no PPAR $\gamma$  activity and can



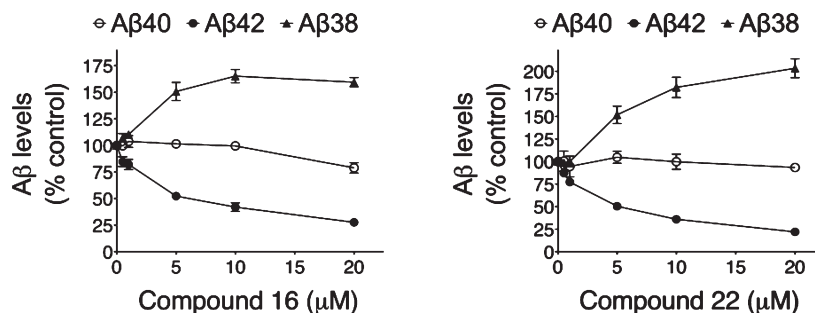


**Figure 3.** GSM activity of compounds **16** and **22**: dose–response curves for A $\beta$ 40, A $\beta$ 42, and A $\beta$ 38 formation.

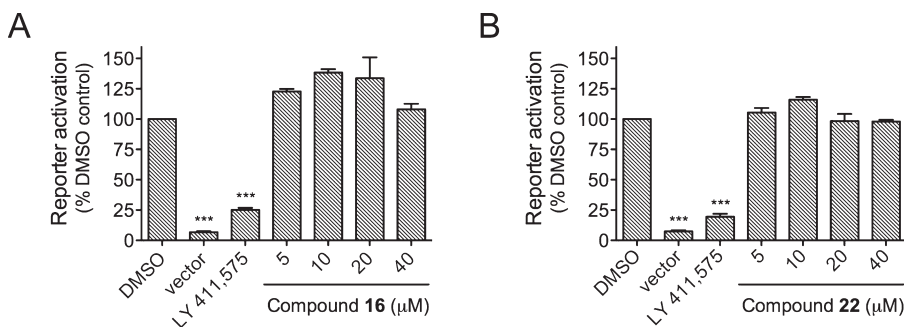


**Figure 4.** Lack of effect of compounds **16** and **22** in the NOTCH reporter gene assay.

thus be described as a conventional GSM. With an  $IC_{50}$  of 29.3  $\mu$ M for A $\beta$ 42 inhibition, compound **10** is somewhat less potent compared to the lead structure. Together, the initial *n*-butyl chain (**8**) turned out to have the optimal chain length in  $\alpha$ -position for dual modulation of  $\gamma$ -secretase and PPAR $\gamma$ . Interestingly, it was possible to modify the activity profile toward a conventional GSM by the introduction of a bulky phenyl moiety in  $\alpha$ -position to the carboxylic acid.

On the basis of previous studies where we have assessed the influence of the stereochemical configuration of some  $\alpha$ -alkyl substituted pirinixic acid derivatives on PPAR activity,<sup>43</sup> we decided to investigate the stereochemical impact on the biological activity of **8**. We have separated **8** into its single enantiomers (**8c** and **8d**) using enantioselective preparative HPLC.<sup>44</sup> While the (*R*)-enantiomer **8c** ( $IC_{50}(A\beta 42) = 21.5 \mu$ M) showed slightly superior activity compared to the (*S*)-enantiomer (**8d**) ( $IC_{50}(A\beta 42) = 32.6 \mu$ M) on  $\gamma$ -secretase, the results on PPAR $\gamma$  were vice versa (**8c**, 22% activation at 10  $\mu$ M; **8d**,  $EC_{50} = 10.4 \mu$ M). In summary, we were not able to identify any superior biological activity of one enantiomer. Thus, the stereocenter in the  $\alpha$ -position of the carboxylic acid does not cause a significant impact on  $\gamma$ -secretase and PPAR $\gamma$  activity.

Most space for structural modifications is provided by the two ether substituents of the central pyrimidine core of lead structure **8**. First, we elongated and shortened the aliphatic spacer between the two ether moieties and the phenyl residues (compounds **11**–**13**). Compound **11** ( $IC_{50}(A\beta 42) = 25.2 \mu$ M) with a shorter methylene and compound **13** with a longer butylene spacer were almost equipotent on  $\gamma$ -secretase compared to **8**, whereas the elongation to a propylene spacer (**12**) led to a decreased potency. In regard to PPAR $\gamma$  activation, the methylene analogue **11** showed a substantially decreased activity. The elongation to propylene and butylene spacers (**12** and **13**) did not cause considerable changes in PPAR $\gamma$  activity.

Second, we introduced different substituents in para-position of both phenyl moieties based on lead structure **8**. Methyl

(compound **14**) and methoxy (**15**) substituents increased GSM activity with methyl ( $IC_{50}(A\beta 42) = 13.0 \mu$ M) being slightly superior to methoxy ( $IC_{50}(A\beta 42) = 19.3 \mu$ M). Further improvement of A $\beta$ 42 inhibition was finally achieved by introduction of trifluoromethyl (**16**) ( $IC_{50}(A\beta 42) = 6.0 \mu$ M, Figure 3) and trifluoromethoxy moieties (**17**) ( $IC_{50}(A\beta 42) = 8.6 \mu$ M), which belong to the most potent GSMs from this series. Compounds **16** and **17** modulate PPAR $\gamma$  with an  $EC_{50}$  of about 10  $\mu$ M. In contrast to these four derivatives, introduction of nitro (**18**), cyano (**19**), and the bioisosteric replacement of both benzenes by thiophene (**20**) caused a clear decrease of GSM activity with  $IC_{50}$  values above 30  $\mu$ M.

Finally, we replaced the phenyl moieties by aliphatic rings of various sizes. Substitution with cycloheptyl (**21**), cyclohexyl (**22**), and cyclopentyl (**23**) moieties improved the potency regarding inhibition of GSM activity with  $IC_{50}$  values for A $\beta$ 42 in the low micromolar range. The cyclopentyl ( $IC_{50}(A\beta 42) = 17.2 \mu$ M) and cycloheptyl ( $IC_{50}(A\beta 42) = 11.3 \mu$ M) derivatives showed considerable activity. However, the most active compound is the cyclohexyl derivative **22** ( $IC_{50}(A\beta 42) = 5.1 \mu$ M), which represents the most potent GSM presented in this study (Figure 3). Further size restriction to cyclopropyl (**24**) as well as ring-opening of the cyclopropyl (isopentyl-substituted **25**) was detrimental with  $IC_{50} > 28 \mu$ M. Within this series, PPAR $\gamma$  activity remained in the range between 4 and 11  $\mu$ M (**21**–**25**). The largest cycloheptyl substituent (**21**) caused a complete loss of PPAR $\gamma$  activity, thereby representing the second conventional GSM besides  $\alpha$ -phenyl substituted **10**.

**NOTCH Processing.** Potential effects on NOTCH processing were examined for compounds **16** and **22** that displayed the highest GSM activity with an established reporter assay.<sup>38</sup> Treatment of cells with the  $\gamma$ -secretase inhibitor L-685,458 or replacement of the plasmid encoding NOTCH with an empty vector caused a dramatic decrease in reporter activity as expected (Figure 4). However, treatment of cells with 5–40  $\mu$ M compounds **16** (Figure 4A) and **22** (Figure 4B)

**Table 2.** COX Inhibition of Compounds 6–25<sup>a</sup>

compd	remaining activity ± SD at 10 μM (%)		compd	remaining activity ± SD at 10 μM (%)	
	COX-1	COX-2		COX-1	COX-2
<b>6</b>	91.8 ± 5.5	91.7 ± 15.6	<b>15</b>	72.8 ± 29.1	94.6 ± 33.0
<b>7</b>	84.6 ± 5.5	56.9 ± 1.4	<b>16</b>	54.4 ± 23.6	69.0 ± 27.7
<b>8</b>	64.2 ± 24.8	90.9 ± 28.8	<b>17</b>	73.0 ± 11.5	75.8 ± 8.7
	IC <sub>50</sub> = 18.7 μM	IC <sub>50</sub> > 40 μM		IC <sub>50</sub> = 16.9 μM	IC <sub>50</sub> > 40 μM
<b>8c</b>	73.9 ± 15.8	98.5 ± 11.1	<b>18</b>	82.1 ± 12.2	91.6 ± 14.6
<b>8d</b>	83.5 ± 12.6	92.8 ± 2.1	<b>19</b>	88.8 ± 16.6	82.6 ± 24.3
<b>9</b>	61.8 ± 17.0	63.8 ± 16.8	<b>20</b>	76.6 ± 6.9	102.4 ± 16.9
<b>10</b>	72.2 ± 13.3	86.0 ± 21.8	<b>21</b>	56.1 ± 8.8	50.1 ± 9.3
<b>11</b>	88.9 ± 21.3	61.6 ± 2.4	<b>22</b>	52.7 ± 11.1	49.5 ± 18.5
				IC <sub>50</sub> = 13.4 μM	IC <sub>50</sub> = 10.9 μM
<b>12</b>	78.8 ± 14.9	51.9 ± 11.3	<b>23</b>	68.2 ± 6.9	84.7 ± 3.5
<b>13</b>	78.8 ± 14.0	53.9 ± 14.2	<b>24</b>	97.7 ± 17.4	87.9 ± 5.8
<b>14</b>	57.2 ± 12.7	93.3 ± 20.0	<b>25</b>	72.4 ± 31.3	80.5 ± 25.5

<sup>a</sup>IC<sub>50</sub> values were determined for compounds **8**, **16**, and **22**.

did not reduce reporter activity, indicating that these potent dual  $\gamma$ -secretase/PPAR $\gamma$  modulators did not affect NOTCH processing or signaling in this concentration range (Figure 4).

**Cytotoxicity.** Cytotoxicity of all novel analogues was determined in the concentration range between 10 and 100 μM using Alamar blue reagent and is summarized in the Supporting Information. With one exception (i.e., compound **16**), none of the compounds displayed detectable cytotoxicity up to 60 μM. Compound **16** showed 25% cytotoxicity at 60 μM without significant effects at 40 μM, which is 6- to 7-fold above its IC<sub>50</sub> value for A $\beta$ 42 inhibition (6.0 μM).

**COX Inhibition.** Most NSAIDs-type GSMs such as indomethacin inhibit COX-1 and COX-2 with IC<sub>50</sub> values in the nanomolar range (Figure 1). Consequently, COX-related side effects are a major obstacle for their long-term clinical use. Thus, one of the main objectives of this study was to develop a potent dual  $\gamma$ -secretase/PPAR $\gamma$  modulator with substantially weaker COX inhibitory activity compared to NSAID-type GSMs. Inhibition of isolated ovine COX-1 and human recombinant COX-2 is summarized in Table 2 and presented as remaining activity at 10 μM. Importantly, all novel compounds synthesized within this study were weak COX-1 and COX-2 inhibitors with at least half-maximal remaining activities at 10 μM. Furthermore, we have determined IC<sub>50</sub> values for lead compound **8** as well as for the most active compounds **16** and **22**. Compound **8** displays moderate COX-1 inhibition with an IC<sub>50</sub> of 18.7 μM and very weak COX-2 inhibition (IC<sub>50</sub> > 40 μM). The introduction of cyclohexyl residues (compound **22**: IC<sub>50</sub>(A $\beta$ 42) = 5.1 μM, EC<sub>50</sub>(PPAR $\gamma$ ) = 6.6 μM) improved dual  $\gamma$ -secretase/PPAR $\gamma$  activity but also caused slightly increased COX-1 inhibition and COX-2 inhibition (IC<sub>50</sub>(COX-1) = 13.4 μM, IC<sub>50</sub>(COX-2) = 10.9 μM). *p*-Trifluoromethylphenyl-substituted **16** (IC<sub>50</sub>(A $\beta$ 42) = 6.0 μM, EC<sub>50</sub>(PPAR $\gamma$ ) = 11 μM) shows weaker COX-1 inhibitory activity (IC<sub>50</sub> = 16.9 μM) while sparing inhibition of COX-2. These results suggest an advantage of *p*-trifluoromethylphenyl over cyclohexyl substitution in regard to COX selectivity. In summary, the introduction of *p*-trifluoromethylphenyl residues (**16**) resulted in the most favorable pharmacological profile with superiority of GSM activity versus COX-inhibition.

## Discussion

This study presents the successful establishment of a novel and robust scaffold for potent dual  $\gamma$ -secretase/PPAR $\gamma$  modulators. The structural starting point was our initial hit **8**,

which was used as a template for structural variations with a special focus on the lipophilic parts of the molecule. Our SAR studies revealed clear SAR in  $\alpha$ -position to the carboxylic acid, where the introduction of a *n*-butyl chain led to the highest GSM activity. In contrast, the lipophilic backbone of the molecule showed high tolerance toward structural modification. Introduction of different aromatic and aliphatic moieties linked by aliphatic spacers was well tolerated and showed activity on both  $\gamma$ -secretase and PPAR $\gamma$ . Substantial improvement was finally achieved by the replacement of the two phenyl residues with cyclohexyl (**22**) or by the attachment of *p*-trifluoromethyl substituents (**16**). Cyclohexyl-substituted **22** showed nearly equipotent activities in the low micromolar range with an A $\beta$ 42 IC<sub>50</sub> of 5.1 μM and a PPAR $\gamma$  EC<sub>50</sub> of 6.6 μM. The *p*-trifluoromethyl derivative had comparable GSM activity with an A $\beta$ 42 IC<sub>50</sub> of 6.0 μM, slightly weaker PPAR $\gamma$  activity with an EC<sub>50</sub> of 11 μM but the more promising selectivity profile (IC<sub>50</sub>(COX-1) = 16.9 μM, IC<sub>50</sub>(COX-2) > 40 μM). Importantly, these compounds did not impair NOTCH processing in the noncytotoxic concentration range.

Taken together, this series represents the first class of compounds described as dual  $\gamma$ -secretase/PPAR $\gamma$  modulators. By structural modifications we were able to cover the whole range from selective GSMs to equipotent and low micromolar active dual  $\gamma$ -secretase/PPAR $\gamma$  modulators. A major liability of the initially discovered GSMs in the class of NSAIDs are COX-associated gastrointestinal and cardiovascular side effects. These side effects most likely preclude the long-term use of A $\beta$ 42-lowering NSAIDs to prevent AD.<sup>45</sup> However, the here presented compounds show substantially lower COX inhibition compared to A $\beta$ 42-lowering NSAIDs such as ibuprofen (Figure 1). We propose that dual  $\gamma$ -secretase/PPAR $\gamma$  modulators could provide a promising strategy to address the increased dementia risk in patients with insulin resistance and type 2 diabetes. In these individuals, dual-active molecules might ameliorate the deleterious effects associated with insulin resistance by activation of PPAR $\gamma$  and further confront the elevated risk for AD by modulating  $\gamma$ -secretase activity and lowering A $\beta$ 42 levels in brain.

## Experimental Section

**Compounds and Chemistry.** The structures of compounds **6**–**25** were confirmed by <sup>1</sup>H NMR, <sup>13</sup>C NMR, and mass spectrometry (ESI). The purities of the final compounds described here were determined by combustion analysis and are 95% or

higher. Commercial chemicals and solvents were reagent grade and used without further purification.  $^1\text{H}$  and  $^{13}\text{C}$  NMR spectra were measured in  $\text{DMSO-}d_6$  or  $\text{CDCl}_3$  on a Bruker ARX 300 ( $^1\text{H}$  NMR) and AC 200 E ( $^{13}\text{C}$  NMR) spectrometer. Chemical shifts are reported in parts per million (ppm) using tetramethylsilane (TMS) as internal standard. Mass spectra were obtained on a Fissous Instruments VG Platform 2 spectrometer measuring in the positive- or negative-ion mode (ESI-MS system). Combustion analysis was performed by the Microanalytical Laboratory of the Institute of Organic Chemistry and Chemical Biology, Goethe University Frankfurt, on a Foss Heraeus CHNO rapid elemental analyzer (for details see the Supporting Information).

The general synthesis of compounds (Scheme 2) follows the routes described recently.<sup>34</sup> The synthetic procedure is described representatively for compounds **8** and **16**. Detailed synthesis and analytical data of all compounds are provided in the Supporting Information.

**Step i.** 2-Thiobarbituric acid (4.33 g/30 mmol, 1 equiv) was suspended in anhydrous DMF (~30 mL, quantum satis), and triethylamine (4.56 g/45 mmol, 1.5 equiv) was added. Heating to 80–90 °C yielded a clear solution, to which ethyl 2-bromohexanoate (10.05 g/45 mmol, 1.5 equiv) was added dropwise. After being stirred for 4 h at 80 °C (TLC control), the reaction mixture was quenched with at least four parts of water and extracted three times with ethyl acetate. Solvent evaporation of the organic phase yielded the crude product, which was purified by column chromatography using hexane/ethyl acetate to obtain **8a** as a white solid. Yield: 55.9% (4.8 g).

**Step iia.** Compound **8b** was prepared under Williamson conditions. The precursor from step i (1.2 g/4.19 mmol, 1 equiv) and (2-bromoethyl)benzene (1.63 g/8.8 mmol, 2.1 equiv) were suspended in anhydrous DMF (quantum satis) and heated to 80–90 °C.  $\text{K}_2\text{CO}_3$  (1.34 g/9.72 mmol, 2.32 equiv) was added, and the resulting suspension was stirred for 9 h. After completion of the reaction (TLC control), DMF was evaporated in vacuo at 60 °C and the remaining solid was diluted with water. After neutralization to pH 7, the aqueous phase was extracted two times with ethyl acetate. The combined organic fractions were washed with brine and dried over  $\text{MgSO}_4$ . Solvent evaporation gave the crude product, which was purified by column chromatography using hexane/ethyl acetate to yield **8b** as clear oil. Yield: 63.7% (1.32 g).

**Step iib.** Compound **16b** was synthesized under Mitsunobu conditions. Thereby, **8a** (0.45 g/1.6 mmol, 1 equiv), 4-trifluoromethylphenylethanol (0.6 g/3.2 mmol, 2.1 equiv), and triphenylphosphine (1.2 g/4.57 mmol, 2.5 equiv) were dissolved in anhydrous THF and stirred under argon atmosphere with ice bath cooling. Diethylazodicarboxylate (DEAD, 0.78 g/4.57 mmol, 2.5 equiv) diluted in 5 mL of THF was added dropwise via a syringe, and the solution was stirred for 1 h until the reaction was completed (TLC control). Subsequently, THF was evaporated and the remaining residue was purified by column chromatography using hexane/ethyl acetate to yield **16b** as clear oil in 64.3% (0.64 g) yield.

**Step iii.** The corresponding ester (**8b** (0.84 g/1.7 mmol, 1 equiv) or **16b** (0.4 g/0.6 mmol, 0.6 equiv)) was dissolved in a mixture of 5 mL of THF/10 mL of MeOH, and a solution of  $\text{LiOH}\cdot\text{H}_2\text{O}$  (3 equiv) in 3 mL of  $\text{H}_2\text{O}$  was added. After the mixture was stirred at 50 °C until saponification was completed, the solvent was removed and the residue was dissolved in water (under heating; if necessary, low amounts of MeOH were added). The solution was acidified with diluted hydrochloric acid. The formed precipitate (**8**) was filtered, washed to neutrality with water, and then washed with *n*-hexane. Recrystallization from *n*-hexane/ethyl acetate yielded compound **8** as a white solid. Yield: 78.4% (0.62 g).

In the case of compound **16**, the precipitate formed after addition of diluted hydrochloric acid was oily. To purify the crude product, the residue was extracted with ethyl acetate and

separated by column chromatography using *n*-hexane/ethyl acetate. Yield: 92.2% (0.35 g).

**Ethyl 2-(4,6-Dihydroxypyrimidin-2-ylthio)hexanoate (8a).** White solid, mp 173 °C.  $^1\text{H}$  NMR (300.13 MHz,  $(\text{CD}_3)_2\text{SO}$ ):  $\delta$  = 0.82–0.87 (t, 3H,  $J$  = 6.9 Hz,  $\text{CH}_3$ -Bu), 1.14–1.19 (t, 3H,  $J$  = 7.1 Hz,  $-\text{CH}_3$ ), 1.28–1.31 (m, 4H,  $\text{CH}_2$ -Bu), 1.72–1.92 (m, 2H,  $\text{CH}_2$ -Bu), 4.08–4.15 (q, 2H,  $J$  = 7.1 Hz,  $\text{OCH}_2$ ), 4.47–4.52 (t, 1H,  $J$  = 7.1 Hz, S-CH), 5.22 (s, 1H, Pyr-5H), 11.75 (s, br, 2H, Pyr-OH).  $^{13}\text{C}$  NMR (75.44 MHz,  $(\text{CD}_3)_2\text{SO}$ ):  $\delta$  = 13.63 ( $-\text{CH}_3$ ), 13.89 ( $\text{CH}_3$ -Bu), 21.59 ( $\text{CH}_2$ -Bu), 28.49 ( $\text{CH}_2$ -Bu), 31.27 ( $\text{CH}_2$ -Bu), 46.39 (S-CH), 61.06 ( $\text{OCH}_2$ ), 85.62 (Pyr-C<sub>5</sub>), 167.79 (Pyr-C<sub>2</sub>), 170.86 (COO). MS (ESI<sup>-</sup>):  $m/e$  = 284.9 [ $\text{M} - 1$ ]<sup>-</sup>.

**Ethyl 2-(4,6-Diphenethoxypyrimidin-2-ylthio)hexanoate (8b).** Clear oil.  $^1\text{H}$  NMR (250.13 MHz,  $(\text{CD}_3)_2\text{SO}$ ):  $\delta$  = 0.82 (t, 3H,  $J$  = 7.1 Hz,  $\text{CH}_3$ -Bu), 1.05 (t, 3H,  $J$  = 7.1 Hz,  $-\text{CH}_3$ ), 1.26–1.34 (m, 4H,  $\text{CH}_2$ -Bu), 1.74–1.91 (m, 2H,  $\text{CH}_2$ -Bu), 2.98 (t, 4H,  $J$  = 7.1 Hz, Ph- $\text{CH}_2$ ), 4.11 (q, 2H,  $J$  = 7.1 Hz,  $\text{OCH}_2$ ), 4.32–4.48 (m, 5H, S- $\text{CH}_2$  + Pyr-O- $\text{CH}_2$ ), 5.89 (s, 1H, Pyr-5H), 7.19–7.32 (m, 10H, Ph-H).  $^{13}\text{C}$  NMR (75.44 MHz,  $(\text{CD}_3)_2\text{SO}$ ):  $\delta$  = 13.63 ( $\text{CH}_3$ -Bu), 13.83 ( $-\text{CH}_3$ ), 21.60 ( $\text{CH}_2$ -Bu), 28.79 ( $\text{CH}_2$ -Bu), 30.72 ( $\text{CH}_2$ -Bu), 34.43 (2C, Ph- $\text{CH}_2$ ), 47.13 (S- $\text{CH}_2$ ), 60.90 ( $\text{OCH}_2$ ), 67.12 (2C, Pyr-O- $\text{CH}_2$ ), 86.01 (Pyr-C<sub>5</sub>), 126.34 (2C, Ph-C<sub>4</sub>), 128.12 (4C, Ph-C<sub>2</sub> +  $-\text{C}_6$ ), 128.61 (4C, Ph-C<sub>3</sub> +  $-\text{C}_5$ ), 137.80 (2C, Ph-C<sub>1</sub>), 168.54 (Pyr-C<sub>2</sub>), 170.07 (2C, Pyr-C<sub>4</sub> +  $-\text{C}_6$ ), 171.35 (COO). MS (ESI<sup>+</sup>):  $m/e$  = 495.2 [ $\text{M} + \text{H}$ ]<sup>+</sup>.

**Ethyl 2-(4,6-Bis(4-(trifluoromethyl)phenethoxy)pyrimidin-2-ylthio)hexanoate (16b).** Clear oil.  $^1\text{H}$  NMR (300.13 MHz,  $(\text{CD}_3)_2\text{SO}$ ):  $\delta$  = 0.79–0.83 (t, 3H,  $J$  = 7.1 Hz,  $\text{CH}_3$ -Bu), 1.02–1.06 (t, 3H,  $J$  = 7.0 Hz,  $-\text{CH}_3$ ), 1.29–1.40 (m, 4H,  $\text{CH}_2$ -Bu), 1.84–1.92 (m, 2H,  $\text{CH}_2$ -Bu), 3.07–3.11 (t, 4H,  $J$  = 6.6 Hz, Ph- $\text{CH}_2$ ), 3.97–4.08 (m, 2H,  $\text{OCH}_2$ ), 4.29–4.35 (t, 1H,  $J$  = 7.2 Hz, S-CH), 4.47–4.53 (m, 4H, Pyr-O- $\text{CH}_2$ ), 5.89 (s, 1H, Pyr-5H), 7.49–7.52 (d, 4H,  $J$  = 8.0 Hz, Ph-C<sub>2</sub> +  $-\text{C}_6\text{H}$ ), 7.63–7.66 (d, 4H,  $J$  = 8.1 Hz, Ph-C<sub>3</sub> +  $-\text{C}_5\text{H}$ ).  $^{13}\text{C}$  NMR (75.44 MHz,  $(\text{CD}_3)_2\text{SO}$ ):  $\delta$  = 13.60 ( $\text{CH}_3$ -Bu), 14.07 ( $-\text{CH}_3$ ), 21.60 ( $\text{CH}_2$ -Bu), 28.79 ( $\text{CH}_2$ -Bu), 30.64 ( $\text{CH}_2$ -Bu), 34.15 (2C, Ph- $\text{CH}_2$ ), 47.16 (S-CH), 60.88 ( $\text{OCH}_2$ ), 66.59 (2C, Pyr-O- $\text{CH}_2$ ), 86.06 (Pyr-C<sub>5</sub>), 125.11 (4C, Ph-C<sub>3</sub> +  $-\text{C}_5$ ), 126.13–127.35 (2C, Ph-CF<sub>3</sub>), 129.71 (4C, Ph-C<sub>2</sub> +  $-\text{C}_6$ ), 143.01 (2C, Ph-C<sub>1</sub>), 168.59 (Pyr-C<sub>2</sub>), 169.99 (2C, Pyr-C<sub>4</sub> +  $-\text{C}_6$ ), 171.31 (COO). MS (ESI<sup>+</sup>):  $m/e$  = 631.6 [ $\text{M} + 1$ ]<sup>+</sup>.

**2-(4,6-Diphenethoxypyrimidin-2-ylthio)hexanoic Acid (8).** White solid, mp 99 °C.  $^1\text{H}$  NMR (300.13 MHz,  $(\text{CD}_3)_2\text{SO}$ ):  $\delta$  = 0.81 (t, 3H,  $J$  = 7.1 Hz,  $\text{CH}_3$ -Bu), 1.23–1.38 (m, 4H,  $\text{CH}_2$ -Bu), 1.78–1.90 (m, 2H,  $\text{CH}_2$ -Bu), 2.98 (t, 4H,  $J$  = 6.9 Hz, Ph- $\text{CH}_2$ ), 4.29 (t, 1H,  $J$  = 7.2 Hz, S-CH), 4.46 (t, 4H,  $J$  = 6.9 Hz, Pyr-O- $\text{CH}_2$ ), 5.87 (s, 1H, Pyr-5H), 7.18–7.32 (m, 10H, Ph-H).  $^{13}\text{C}$  NMR (75.44 MHz,  $(\text{CD}_3)_2\text{SO}$ ):  $\delta$  = 13.70 ( $\text{CH}_3$ -Bu), 21.71 ( $\text{CH}_2$ -Bu), 28.92 ( $\text{CH}_2$ -Bu), 31.09 ( $\text{CH}_2$ -Bu), 34.44 (2C, Ph- $\text{CH}_2$ ), 47.61 (S- $\text{CH}_2$ ), 67.08 (2C, Pyr-O- $\text{CH}_2$ ), 85.87 (Pyr-C<sub>5</sub>), 126.31 (2C, Ph-C<sub>4</sub>), 128.30 (4C, Ph-C<sub>2</sub> +  $-\text{C}_6$ ), 128.84 (4C, Ph-C<sub>3</sub> +  $-\text{C}_5$ ), 137.88 (2C, Ph-C<sub>1</sub>), 169.01 (Pyr-C<sub>2</sub>), 170.03 (2C, Pyr-C<sub>4</sub> +  $-\text{C}_6$ ), 172.70 (COOH). MS (ESI<sup>+</sup>):  $m/e$  = 467.0 [ $\text{M} + \text{H}$ ]<sup>+</sup>.

**2-(4,6-Bis(4-(trifluoromethyl)phenethoxy)pyrimidin-2-ylthio)hexanoic Acid (16).** Yellow oil.  $^1\text{H}$  NMR (300.13 MHz,  $(\text{CD}_3)_2\text{SO}$ ):  $\delta$  = 0.78–0.83 (t, 3H,  $J$  = 7.1 Hz,  $\text{CH}_3$ -Bu), 1.22–1.37 (m, 4H,  $\text{CH}_2$ -Bu), 1.74–1.92 (m, 2H,  $\text{CH}_2$ -Bu), 3.06–3.11 (t, 4H,  $J$  = 6.6 Hz, Ph- $\text{CH}_2$ ), 4.27–4.30 (t, 1H,  $J$  = 7.1 Hz, S-CH), 4.48–4.53 (t, 4H,  $J$  = 6.6 Hz, Pyr-O- $\text{CH}_2$ ), 5.87 (s, 1H, Pyr-5H), 7.49–7.52 (d, 4H,  $J$  = 8.0 Hz, Ph-C<sub>2</sub> +  $-\text{C}_6\text{H}$ ), 7.63–7.66 (d, 4H,  $J$  = 8.0 Hz, Ph-C<sub>3</sub> +  $-\text{C}_5\text{H}$ ), 12.82 (s, br, 1H, COOH).  $^{13}\text{C}$  NMR (75.44 MHz,  $(\text{CD}_3)_2\text{SO}$ ):  $\delta$  = 13.64 ( $\text{CH}_3$ -Bu), 21.67 ( $\text{CH}_2$ -Bu), 28.92 ( $\text{CH}_2$ -Bu), 30.91 ( $\text{CH}_2$ -Bu), 34.16 (2C, Ph- $\text{CH}_2$ ), 47.46 (S-CH), 66.54 (2C, Pyr-O- $\text{CH}_2$ ), 85.97 (Pyr-C<sub>5</sub>), 124.99 (4C, Ph-C<sub>3</sub> +  $-\text{C}_5$ ), 125.14–127.74 (2C, Ph-CF<sub>3</sub>), 129.69 (4C, Ph-C<sub>2</sub> +  $-\text{C}_6$ ), 143.06 (2C, Ph-C<sub>1</sub>), 168.95 (Pyr-C<sub>2</sub>), 169.97 (2C, Pyr-C<sub>4</sub> +  $-\text{C}_6$ ), 172.23 (COOH). MS (ESI<sup>-</sup>):  $m/e$  = 601.4 [ $\text{M} - 1$ ]<sup>-</sup>.

**PPAR Transactivation Assay.** COS7 cells were grown in DMEM supplemented with FCS, sodium pyruvate, and penicillin/streptomycin at 37 °C and 5%  $\text{CO}_2$ . The day before transfection, cells were seeded in 96-well plates at a density of 30 000 cells



per well. Transient transfection was carried out by Lipofectamine 2000 reagent (Invitrogen) according to the manufacturer's protocol with pFR-Luc (Stratagene), pRL-SV40 (Promega), and the Gal4-fusion receptor plasmids (pFA-CMV-hPPAR-LBD) of the respective subtype. At 5 h after transfection, the medium was changed to DMEM without phenol red and FCS, containing 0.1% DMSO and the respective concentrations of the test compounds.

Following overnight incubation with the test compounds, cells were assayed for reporter gene activity using Dual-Glo luciferase assay system (Promega) according to the manufacturer's protocol. Luminescence was measured with a GENios Pro luminometer (Tecan Deutschland GmbH, Crailsheim, Germany). Each concentration of the compounds was tested in triplicate wells, and each experiment was repeated independently at least three times. Normalization for transfection efficacy and cell growth was done by division of the firefly luciferase data by renilla luciferase data resulting in relative light units. Activation factors were obtained by dividing by DMSO control. EC<sub>50</sub> and standard deviation values were calculated by mean values of at least three determinations by SigmaPlot 2001 (Systat Software GmbH, Erkrath, Germany) using a four-parameter logistic regression. All compounds were evaluated by comparison of the achieved maximum effect to that of the reference compound (pioglitazone for PPAR $\gamma$ , GW 7647 for PPAR $\alpha$ , and L165,041 for PPAR $\delta$  each with 1  $\mu$ M).

**Determination of  $\gamma$ -Secretase Modulator Activity.** To characterize the GSM activity of novel analogues, their effects on the generation of A $\beta$ 40, A $\beta$ 42, and A $\beta$ 38 peptides were determined in a previously described cell-based ELISA assay with modifications.<sup>37</sup> CHO cells with stable overexpression of wild type human amyloid precursor protein and wild type human presenilin-1<sup>37</sup> were maintained in DMEM supplemented with 10% FBS and treated in 96-well plates for 24 h with increasing concentrations of the respective compounds or DMSO vehicle. Culture media were collected and analyzed by ELISA as follows: monoclonal antibody IC16 raised against amino acids 1–15 of the A $\beta$  sequence was used as a capture antibody.<sup>46</sup> To distinguish different A $\beta$  species, C-terminal antibodies specific for A $\beta$ 40, A $\beta$ 42, and A $\beta$ 38 labeled with horseradish peroxidase (HRP) using the Pierce EZ-Link Plus activated peroxidase kit (Thermo Fisher Scientific) were used for detection. The 96-well high-binding microtiter plates were coated overnight at 4 °C with capture antibody IC16 diluted 1:250 in PBS, pH 7.2. Capture antibody was removed, and conditioned media samples (10  $\mu$ L for detection of A $\beta$ 40, 100  $\mu$ L for A $\beta$ 42, 50  $\mu$ L for A $\beta$ 38) or standard peptides were loaded. HRP-coupled detection antibodies diluted in assay buffer (PBS containing 0.05% Tween-20, 1% BSA) were added to each well and incubated overnight at 4 °C. Plates were washed 3 times with PBS containing 0.05% Tween-20 and once with PBS. Then 50  $\mu$ L of TMB ultrasubstrate (Thermo Fisher Scientific) was added and incubated for 1–10 min at room temperature in the dark, and the reaction was stopped by adding 50  $\mu$ L of 2 M H<sub>2</sub>SO<sub>4</sub>. Absorbance at 450 nm was recorded with a Paradigm microplate reader (Beckman-Coulter). Synthetic A $\beta$ 40, A $\beta$ 42, and A $\beta$ 38 peptides (Bachem AG) were used to generate standard curves. These A $\beta$  peptides were solubilized in DMSO at 1 mg/mL, aliquoted, and stored frozen at –80 °C. Immediately before use, peptides were diluted in assay buffer to 250–3000 pg/mL. Triplicate measurements from each drug concentration were averaged and normalized to DMSO control condition. For calculation of IC<sub>50</sub> values, cells were treated with eight increasing concentrations of each compound, and a nonlinear curve fit with variable slope model was applied to the results from two to four independent experiments. Statistics were performed using GraphPad Prism (GraphPad Software).

**NOTCH Reporter Assay.** The NOTCH reporter assay was performed as described.<sup>38</sup> In brief, subconfluent CHO cells were transiently transfected in 96-well plates with plasmid pCDNA3-Notch- $\Delta$ E-GVP encoding truncated NOTCH fused to a Gal4

DNA-binding/VP16 transactivation domain and the MH100 reporter plasmid encoding firefly luciferase under the UAS promoter (50 ng each) using GeneJuice transfection reagent (Merck Chemicals Ltd.). Co-transfection of the MH100 reporter with empty pCDNA3 plasmid served as a negative control. Then 5 ng of plasmid pRL-TK encoding renilla luciferase was added to the plasmid mix to control for transfection efficiency. At 24 h after the transfection, cells were treated for an additional 24 h with increasing concentrations of the compounds **16** and **22**, 0.5  $\mu$ M  $\gamma$ -secretase inhibitor LY-411575, or DMSO vehicle. The cells were then lysed, and firefly and renilla luciferase activities were quantified using the Dual Glo luciferase assay system (Promega) and a PARADIGM microplate reader (Beckman-Coulter). Normalization for transfection efficacy and cell growth was achieved by dividing the firefly luciferase values by the renilla luciferase values. Percent activation of the reporter was then calculated by normalization of triplicate measurements from each condition to the DMSO control values. Unpaired *t* test analysis was performed from two independent experiments using GraphPad Prism: \*\*\*, *p* < 0.001.

**Cytotoxicity Assay.** CHO cells with stable overexpression of wild type human amyloid precursor protein and wild type human presenilin-1 were seeded at low density in 96-well plates (4000 cells/well) and cultured for 24 h. The cells were then treated in duplicate with increasing concentrations (0–100  $\mu$ M) of the respective compounds or DMSO vehicle for an additional 24 h. Cell viability was assessed using the Alamar blue reagent (Invitrogen). Then 20  $\mu$ L of Alamar blue was added to cells cultured in 200  $\mu$ L of medium and incubated overnight. Absorbance was measured with a Paradigm microplate reader (Beckman-Coulter) at 570 nm, using 600 nm as the reference wavelength. The values expressed as percent viability of vehicle control represent averages of two independent experiments.

**Determination of COX Inhibition.** Inhibition of the activities of isolated ovine COX-1 and human recombinant COX-2 was performed as described.<sup>34</sup> Briefly, purified COX-1 (ovine, 50 units) or COX-2 (human recombinant, 20 units) were diluted in 1 mL of reaction mixture containing 100 mM Tris buffer, pH 8, 5 mM glutathione, 5  $\mu$ M hemoglobin, and 100  $\mu$ M EDTA at 4 °C and preincubated with the test compounds for 5 min. Samples were prewarmed for 60 s at 37 °C, and arachidonic acid (5  $\mu$ M for COX-1, 2  $\mu$ M for COX-2) was added to start the reaction. After 5 min at 37 °C, the COX product 12-HHT was extracted and then analyzed by HPLC as described.<sup>41,47</sup>

**Acknowledgment.** We thank Dr. Jan Näslund (Karolinska Institute, Sweden) for the NOTCH reporter plasmids, Dr. Manfred Brockhaus (F. Hoffmann-La Roche Ltd., Switzerland) for carboxyl-terminus-specific A $\beta$  antibodies, Dr. Michael Lämmerhofer (Universität Wien, Austria) for enantioselective separation of compound **8**, and Dr. Boris Schmidt (TU Darmstadt, Germany) for scientific advice. This study was supported by the Competence Network Degenerative Dementias of the Federal Ministry of Education (Grant 01 GI 0718 to S.W.).

**Supporting Information Available:** Chemical synthesis, <sup>1</sup>H and <sup>13</sup>C NMR data of intermediates and final compounds, mass spectrometry, combustion analysis, and cytotoxicity data. This material is available free of charge via the Internet at <http://pubs.acs.org>.

## References

- (1) Brookmeyer, R.; Johnson, E.; Ziegler-Graham, K.; Arrighi, H. M. Forecasting the global burden of Alzheimer's disease. *Alzheimer's Dementia* **2007**, *3*, 186–191.
- (2) Selkoe, D. J. Alzheimer's disease: genes, proteins, and therapy. *Physiol. Rev.* **2001**, *81*, 741–766.



- (3) Walsh, D. M.; Selkoe, D. J.  $A\beta$  oligomers—a decade of discovery. *J. Neurochem.* **2007**, *101*, 1172–1184.
- (4) Citron, M. Strategies for disease modification in Alzheimer's disease. *Nat. Rev. Neurosci.* **2004**, *5*, 677–685.
- (5) Golde, T. E. Disease modifying therapy for AD? *J. Neurochem.* **2006**, *99*, 689–707.
- (6) Barten, D. M.; Meredith, J. E.; Zaczek, R.; Houston, J. G.; Albright, C. F. Gamma-secretase inhibitors for Alzheimer's disease: balancing efficacy and toxicity. *Drugs R&D* **2006**, *7*, 87–97.
- (7) De Strooper, B.; Annaert, W.; Cupers, P.; Saftig, P.; Craessaerts, K.; Mumm, J. S.; Schroeter, E. H.; Schrijvers, V.; Wolfe, M. S.; Ray, W. J.; Goate, A.; Kopan, R. A presenilin-1-dependent gamma-secretase-like protease mediates release of Notch intracellular domain. *Nature* **1999**, *398*, 518–522.
- (8) Wong, G. T.; Manfra, D.; Poulet, F. M.; Zhang, Q.; Josien, H.; Bara, T.; Engstrom, L.; Pinzon-Ortiz, M.; Fine, J. S.; Lee, H. J.; Zhang, L.; Higgins, G. A.; Parker, E. M. Chronic treatment with the gamma-secretase inhibitor LY-411,575 inhibits beta-amyloid peptide production and alters lymphopoiesis and intestinal cell differentiation. *J. Biol. Chem.* **2004**, *279*, 12876–12882.
- (9) Weggen, S.; Eriksen, J. L.; Das, P.; Sagi, S. A.; Wang, R.; Pietrzik, C. U.; Findlay, K. A.; Smith, T. E.; Murphy, M. P.; Bultter, T.; Kang, D. E.; Marquez-Sterling, N.; Golde, T. E.; Koo, E. H. A subset of NSAIDs lower amyloidogenic Abeta42 independently of cyclooxygenase activity. *Nature* **2001**, *414*, 212–216.
- (10) Leuchtenberger, S.; Behr, D.; Weggen, S. Selective modulation of Abeta42 production in Alzheimer's disease: non-steroidal anti-inflammatory drugs (NSAIDs) and beyond. *Curr. Pharm. Des.* **2006**, *12*, 4337–4355.
- (11) Weggen, S.; Rogers, M.; Eriksen, J. NSAIDs: small molecules for prevention of Alzheimer's disease or precursors for future drug development? *Trends Pharmacol. Sci.* **2007**, *28*, 536–543.
- (12) Green, R. C.; Schneider, L. S.; Hendrix, S. B.; Zavitz, K. H.; Swabb, E. Safety and Efficacy of Tarenflurbil in Subjects with Mild Alzheimer's Disease: Results from an 18-Month Multi-Center Phase 3 Trial. Presented at the International Conference on Alzheimer's Disease, Chicago, IL, July 2008; Alzheimer's and Dementia; No. O3-04-01, T165.
- (13) in 't Veld, B. A.; Ruitenber, A.; Hofman, A.; Launer, L. J.; van Duijn, C. M.; Stijnen, T.; Breteler, M. M.; Stricker, B. H. Nonsteroidal antiinflammatory drugs and the risk of Alzheimer's disease. *N. Engl. J. Med.* **2001**, *345*, 1515–1521.
- (14) Vlad, S. C.; Miller, D. R.; Kowall, N. W.; Felson, D. T. Protective effects of NSAIDs on the development of Alzheimer disease. *Neurology* **2008**, *70*, 1672–1677.
- (15) Peretto, J.; La Porta, E. Gamma-secretase modulation and its promise for Alzheimer's disease: a medicinal chemistry perspective. *Curr. Top. Med. Chem.* **2008**, *8*, 38–46.
- (16) Page, R. M.; Baumann, K.; Tomioka, M.; Perez-Revuelta, B. I.; Fukumori, A.; Jacobsen, H.; Flohr, A.; Luebbbers, T.; Ozmen, L.; Steiner, H.; Haass, C. Generation of Abeta 38 and Abeta 42 is independently and differentially affected by FAD-associated presenilin 1 mutations and gamma-secretase modulation. *J. Biol. Chem.* **2008**, *283*, 677–683.
- (17) Jaradat, M. S.; Wongsud, B.; Phornchirasilp, S.; Rangwala, S. M.; Shams, G.; Sutton, M.; Romstedt, K. J.; Noonan, D. J.; Feller, D. R. Activation of peroxisome proliferator-activated receptor isoforms and inhibition of prostaglandin H(2) synthases by ibuprofen, naproxen, and indomethacin. *Biochem. Pharmacol.* **2001**, *62*, 1587–1595.
- (18) Lehmann, J. M.; Lenhard, J. M.; Oliver, B. B.; Ringold, G. M.; Kliewer, S. A. Peroxisome proliferator-activated receptors alpha and gamma are activated by indomethacin and other non-steroidal anti-inflammatory drugs. *J. Biol. Chem.* **1997**, *272*, 3406–3410.
- (19) Lehrke, M.; Lazar, M. A. The many faces of PPARgamma. *Cell* **2005**, *123*, 993–999.
- (20) Landreth, G.; Jiang, Q.; Mandrekar, S.; Heneka, M. PPARgamma agonists as therapeutics for the treatment of Alzheimer's disease. *Neurotherapeutics* **2008**, *5*, 481–489.
- (21) Ho, L.; Qin, W.; Pompl, P. N.; Xiang, Z.; Wang, J.; Zhao, Z.; Peng, Y.; Cambareri, G.; Rocher, A.; Mobbs, C. V.; Hof, P. R.; Pasinetti, G. M. Diet-induced insulin resistance promotes amyloidosis in a transgenic mouse model of Alzheimer's disease. *FASEB J.* **2004**, *18*, 902–904.
- (22) Takeda, S.; Sato, N.; Uchio-Yamada, K.; Sawada, K.; Kunieda, T.; Takeuchi, D.; Kurinami, H.; Shinohara, M.; Rakugi, H.; Morishita, R. Diabetes-accelerated memory dysfunction via cerebrovascular inflammation and Abeta deposition in an Alzheimer mouse model with diabetes. *Proc. Natl. Acad. Sci. U.S.A.* **2010**, *107*, 7036–7041.
- (23) Biessels, G. J.; Staekenborg, S.; Brunner, E.; Brayne, C.; Scheltens, P. Risk of dementia in diabetes mellitus: a systematic review. *Lancet Neurol.* **2006**, *5*, 64–74.
- (24) Luchsinger, J. A. Adiposity, hyperinsulinemia, diabetes and Alzheimer's disease: an epidemiological perspective. *Eur. J. Pharmacol.* **2008**, *585*, 119–129.
- (25) Bernardo, A.; Minghetti, L. PPAR-gamma agonists as regulators of microglial activation and brain inflammation. *Curr. Pharm. Des.* **2006**, *12*, 93–109.
- (26) Combs, C. K.; Johnson, D. E.; Karlo, J. C.; Cannady, S. B.; Landreth, G. E. Inflammatory mechanisms in Alzheimer's disease: inhibition of beta-amyloid-stimulated proinflammatory responses and neurotoxicity by PPARgamma agonists. *J. Neurosci.* **2000**, *20*, 558–567.
- (27) Heneka, M. T.; Sastre, M.; Dumitrescu-Ozimek, L.; Hanke, A.; Dewachter, I.; Kuiperi, C.; O'Banion, K.; Klockgether, T.; Van Leuven, F.; Landreth, G. E. Acute treatment with the PPARgamma agonist pioglitazone and ibuprofen reduces glial inflammation and Abeta1–42 levels in APPV717I transgenic mice. *Brain* **2005**, *128*, 1442–1453.
- (28) Camacho, I. E.; Serneels, L.; Spittaels, K.; Merchiers, P.; Dominguez, D.; De Strooper, B. Peroxisome proliferator-activated receptor gamma induces a clearance mechanism for the amyloid-beta peptide. *J. Neurosci.* **2004**, *24*, 10908–10917.
- (29) Sastre, M.; Dewachter, I.; Rossner, S.; Bogdanovic, N.; Rosen, E.; Borghgraef, P.; Evert, B. O.; Dumitrescu-Ozimek, L.; Thal, D. R.; Landreth, G.; Walter, J.; Klockgether, T.; van Leuven, F.; Heneka, M. T. Nonsteroidal anti-inflammatory drugs repress {beta}-secretase gene promoter activity by the activation of PPAR{gamma}. *Proc. Natl. Acad. Sci. U.S.A.* **2006**, *103*, 443–448.
- (30) Nicolakakis, N.; Aboulkassim, T.; Ongali, B.; Lecrux, C.; Fernandes, P.; Rosa-Neto, P.; Tong, X. K.; Hamel, E. Complete rescue of cerebrovascular function in aged Alzheimer's disease transgenic mice by antioxidants and pioglitazone, a peroxisome proliferator-activated receptor gamma agonist. *J. Neurosci.* **2008**, *28*, 9287–9296.
- (31) Rabiner, E. A.; Tzimopoulou, S.; Cunningham, V. J.; Jeter, B.; Zvartau-Hind, M.; Castiglia, M.; Mistry, P.; Bird, N. P.; Matthews, J.; Whitcher, B.; Nichols, T. E.; Lai, R.; Lotay, N.; Saunders, A.; Reiman, E.; Chen, K.; Gold, M.; Matthews, P. M. Effects of 12 months of treatment with the PPARgamma agonist rosiglitazone on brain glucose metabolism in Alzheimer's disease: a 18F-FDG PET study. *Alzheimer's Dementia* **2009**, *5*, 207.
- (32) Sato, T.; Hanyu, H.; Hirao, K.; Kanetaka, H.; Sakurai, H.; Iwamoto, T. Efficacy of PPAR-gamma agonist pioglitazone in mild Alzheimer disease. *Neurobiol. Aging* [Online early access]. DOI: 10.1016/j.neurobiolaging.2009.10.009. Published Online: Nov 17, 2009.
- (33) Maeshiba, Y.; Kiyota, Y.; Yamashita, K.; Yoshimura, Y.; Motohashi, M.; Tanayama, S. Disposition of the new antidiabetic agent pioglitazone in rats, dogs, and monkeys. *Arzneim. Forsch.* **1997**, *47*, 29–35.
- (34) Koeberle, A.; Zettl, H.; Greiner, C.; Wurglics, M.; Schubert-Zsilavecz, M.; Werz, O. Pirinixic acid derivatives as novel dual inhibitors of microsomal prostaglandin E2 synthase-1 and 5-lipoxygenase. *J. Med. Chem.* **2008**, *51*, 8068–8076.
- (35) Mitsunobu, O. The use of diethyl azodicarboxylate and triphenylphosphine in synthesis and transformation of natural products. *Synthesis* **1981**, *1*, 1–28.
- (36) Zettl, H.; Steri, R.; Lammerhofer, M.; Schubert-Zsilavecz, M. Discovery of a novel class of 2-mercaptohexanoic acid derivatives as highly active PPARalpha agonists. *Bioorg. Med. Chem. Lett.* **2009**, *19*, 4421–4426.
- (37) Czirr, E.; Leuchtenberger, S.; Dorner-Ciossek, C.; Schneider, A.; Jucker, M.; Koo, E. H.; Pietrzik, C. U.; Baumann, K.; Weggen, S. Insensitivity to Abeta 42-lowering non-steroidal anti-inflammatory drugs (NSAIDs) and gamma-secretase inhibitors is common among aggressive presenilin-1 mutations. *J. Biol. Chem.* **2007**, *282*, 24504–24513.
- (38) Karlstrom, H.; Bergman, A.; Lendahl, U.; Naslund, J.; Lundkvist, J. A sensitive and quantitative assay for measuring cleavage of presenilin substrates. *J. Biol. Chem.* **2002**, *277*, 6763–6766.
- (39) Farce, A.; Renault, N.; Chavatte, P. Structural insight into PPAR-gamma ligands binding. *Curr. Med. Chem.* **2009**, *16*, 1768–1789.
- (40) Kukar, T.; Murphy, M. P.; Eriksen, J. L.; Sagi, S. A.; Weggen, S.; Smith, T. E.; Ladd, T.; Khan, M. A.; Kache, R.; Beard, J.; Dodson, M.; Merit, S.; Ozols, V. V.; Anastasiadis, P. Z.; Das, P.; Fauq, A.; Koo, E. H.; Golde, T. E. Diverse compounds mimic Alzheimer disease-causing mutations by augmenting Abeta42 production. *Nat. Med.* **2005**, *11*, 545–550.
- (41) Popescu, L.; Rau, O.; Bottcher, J.; Syha, Y.; Schubert-Zsilavecz, M. Quinoline-based derivatives of pirinixic acid as dual PPAR alpha/gamma agonists. *Arch. Pharm. (Weinheim, Ger.)* **2007**, *340*, 367–371.
- (42) Rau, O.; Syha, Y.; Zettl, H.; Kock, M.; Bock, A.; Schubert-Zsilavecz, M. Alpha-alkyl substituted pirinixic acid derivatives as

- potent dual agonists of the peroxisome proliferator activated receptor alpha and gamma. *Arch. Pharm.* **2008**, *341*, 191–195.
- (43) Zettl, H.; Dittrich, M.; Steri, R.; Proschak, O.; Rau, O.; Steinhilber, D.; Schneider, G.; Lammerhofer, M.; Schubert-Zsilavecz, M. Novel pirinixic acids as PPARalpha preferential dual PPARalpha/gamma agonists. *QSAR Comb. Sci.* **2009**, *28*, 576–586.
- (44) Lammerhofer, M.; Pell, R.; Mahut, M.; Richter, M.; Schiesel, S.; Zettl, H.; Dittrich, M.; Schubert-Zsilavecz, M.; Lindner, W. Enantiomer separation and indirect chromatographic absolute configuration prediction of chiral pirinixic acid derivatives: limitations of polysaccharide-type chiral stationary phases in comparison to chiral anion-exchangers. *J. Chromatogr., A* **2010**, *1217*, 1033–1040.
- (45) Meinert, C. L.; McCaffrey, L. D.; Breitner, J. C. Alzheimer's disease anti-inflammatory prevention trial: design, methods, and baseline results. *Alzheimer's Dementia* **2009**, *5*, 93–104.
- (46) Jager, S.; Leuchtenberger, S.; Martin, A.; Czirr, E.; Wesselowski, J.; Dieckmann, M.; Waldron, E.; Korth, C.; Koo, E. H.; Heneka, M.; Weggen, S.; Pietrzik, C. U. Alpha-secretase mediated conversion of the amyloid precursor protein derived membrane stub C99 to C83 limits Abeta generation. *J. Neurochem.* **2009**, *111*, 1369–1382.
- (47) Kato, M.; Nishida, S.; Kitasato, H.; Sakata, N.; Kawai, S. Cyclooxygenase-1 and cyclooxygenase-2 selectivity of non-steroidal anti-inflammatory drugs: investigation using human peripheral monocytes. *J. Pharm. Pharmacol.* **2001**, *53*, 1679–1685.
- (48) Demello, K. L.; Ricketts, A. P. Cox-2 Selective Carprofen for Treating Pain and Inflammation in Dogs. US2003212123 (A1), 2003.
- (49) Pairet, M., van Ryn, J., Eds. *COX-2 Inhibitors*, 1st ed.; Birkhäuser: Basel, Switzerland, 2004.